

## From Chiral Counterions to Twisted Membranes

Damien Berthier,<sup>†</sup> Thierry Buffeteau,<sup>‡</sup> Jean-Michel Léger,<sup>§</sup> Reiko Oda,<sup>\*,†</sup> and Ivan Huc<sup>\*,†</sup>

Contribution from the Institut Européen de Chimie et Biologie, 16 av. Pey Berland, 33607 Pessac Cedex, France, Laboratoire de Physico-Chimie Moléculaire, 351 cours de la libération, 33405 Talence, France, and Laboratoire de Pharmacochimie, 146 rue Léo Saignat, 33076 Bordeaux, France

Received July 12, 2002

**Abstract:** In membranes, the chirality of the amphiphile constituents is sometimes expressed at a supramolecular scale of nanometers or micrometers. We have recently reported that membranes of nonchiral dicationic  $n-2-n$  amphiphiles can also be chirally twisted upon interacting with chiral tartrate counterions. Here, we demonstrate that the mechanism of the chiral induction by counterions involves specific anion-cation recognition and the induction of conformationally labile chirality in the cations. Single-crystal X-ray diffraction shows that the amphiphilic cations exist as a mixture of chiral conformers. <sup>1</sup>H NMR data establish a specific recognition between tartrate and  $n-2-n$  cations and show that chiral conformers also exist in solution. Circular dichroism (CD) in the UV-vis shows a sharp conformational change of tartrate ions from anti to gauche when bound to the chiral cationic membranes. This is confirmed by CD in the infrared region which also shows concomitant induced CD bands in the vibrations of the  $n-2-n$  amphiphiles. These results represent the first example of the so-called Pfeiffer effect in a membrane. They provide a general framework for designing new tunable membrane systems. Our work also includes the first application of vibrational circular dichroism in the study of chiral conformations of amphiphiles in membranes and demonstrates the very high potential of this technique.

## Introduction

Chiral amphiphiles sometimes assemble into membrane structures with twisted, helical, or cylindrical tubular morphologies that express the chirality of their molecular constituents at a supramolecular scale of micrometers.<sup>1,2</sup> In these mesoscopic objects, the right or left sense of helicity depends directly on the chirality of the amphiphile.<sup>3,4</sup> However, the contribution “per amphiphile” to the membrane chirality is very small. With the

average distance between the amphiphile headgroups being about 0.5–1 nm, thus, thousands of headgroups can be aligned over one turn of a helical membrane.

These objects represent excellent models for studying the emergence of specific shapes at a macroscopic scale through cooperative interactions between a large number of very small building blocks, a topic of fundamental interest in biology. But they also attract considerable interest for the applications that they may have as templates for the helical crystallization of macromolecules<sup>11,5</sup> or, in materials science, as templates for the growth of inorganic replica, be they ceramics, silica, metals, or semiconductors.<sup>6,7</sup>

Several theories have been developed to relate the chiral geometry of bilayer (or multilayer) membranes to the structures

\* To whom correspondence should be addressed. Fax: +33 (0)557 96 22 26. E-mail: i.huc@iecb-polytechnique.u-bordeaux.fr and r.oda@iecb-polytechnique.u-bordeaux.fr.

<sup>†</sup> Institut Européen de Chimie et Biologie.

<sup>‡</sup> Laboratoire de Physico-Chimie Moléculaire.

<sup>§</sup> Laboratoire de Pharmacochimie.

- (1) For example, see: (a) Yager, P.; Schoen, P. E. *Mol. Cryst. Liq. Cryst.* **1984**, *106*, 371–381. (b) Nakashima, N.; Asakuma, S.; Kim, J.-M.; Kunitake, T. *Chem. Lett.* **1984**, 1709–1712. (c) Yamada, K.; Ihara, H.; Ide, T.; Fukumoto, T.; Hirayama, C. *Chem. Lett.* **1984**, 1713–1716. (d) Fuhrhop, J.-H.; Schnieder, P.; Boekema, E.; Helfrich, W. *J. Am. Chem. Soc.* **1988**, *110*, 2861–2867. (e) Yanagawa, H.; Ogawa, Y.; Furuta, H.; Tsuno, K. *J. Am. Chem. Soc.* **1989**, *111*, 4567–4570. (f) Chung, D. S.; Benedek, G. B.; Konikoff, F. M.; Donovan, J. M. *Proc. Natl. Acad. Sci. U.S.A.* **1993**, *90*, 11341–11345. (g) Kulkarni, V. S.; Anderson, W. H.; Brown, R. E. *Biophys. J.* **1995**, *69*, 1976–1986. (h) Giulieri, F.; Guillod, F.; Greiner, J.; Krafft, M.-P.; Riess, J. G. *Chem.—Eur. J.* **1996**, *2*, 1335–1339. (i) Ringler, P.; Müller, W.; Ringsdorf, H.; Brisson, A. *Chem.—Eur. J.* **1997**, *3*, 620–625. (j) Cornelissen, J. J. L. M.; Fisher, M.; Sommedijk, N. A. J. M.; Nolte, R. J. M. *Science* **1998**, *280*, 1427–1430. (k) Sommedijk, N. A. J. M.; Buynters, P. J. J. A.; Akdemir, H.; Geurts, D. G.; Pistorius, A. M. A.; Feiters, M. C.; Nolte, R. J. M.; Zwanenburg, B. *Chem.—Eur. J.* **1998**, *4*, 127–136. (l) Nakasawa, I.; Masuda, M.; Okada, Y.; Hanada, T.; Yase, K.; Asai, M.; Shimizu, T. *Langmuir* **1998**, *15*, 4757–4764. (m) Song, J.; Cheng, Q.; Kopta, S.; Stevens, R. C. *J. Am. Chem. Soc.* **2001**, *123*, 3205–3213.
- (2) (a) Fuhrhop, J.-H.; Helfrich, W. *Chem. Rev.* **1993**, *93*, 1565–1582. (b) Rowan, A. E.; Nolte, R. J. M. *Angew. Chem., Int. Ed.* **1998**, *37*, 63–68.

- (3) When nonchiral amphiphiles assemble into twisted or helical membranes or into tubules, there is no control over the handedness. See: Matsui, H.; Gologan, B. J. *Phys. Chem. B* **2000**, *104*, 8871–8875. Lindsell, W. E.; Preston, P. N.; Seddon, J. M.; Rosair, G. M.; Woodman, T. A. *J. Chem. Mater.* **2000**, *12*, 1572–1576. Singh, A.; Choen, P. E.; Schnur, J. M. *J. Chem. Soc., Chem. Commun.* **1988**, 1222. Giulieri, F.; Krafft, M.-P.; Riess, J. G. *Angew. Chem., Int. Ed. Engl.* **1994**, *33*, 1514–1515. Giulieri, F.; Guillod, F.; Greiner, J.; Krafft, M.-P.; Riess, J. G. *Chem.—Eur. J.* **1995**, *2*, 1335.
- (4) We found one case of a chiral amphiphile that does not exert control over the screw sense of the helical membrane it forms. See: Thomas, B. N.; Corcoran, R. C.; Cotant, C. L.; Lindemann, C. M.; Kirsch, J. E.; Persichini, P. J. *J. Am. Chem. Soc.* **1998**, *120*, 12178–12186. Thomas, B. N.; Lindemann, C. M.; Clark, N. A. *Phys. Rev. E* **1999**, *59*, 3040–3047.
- (5) Wilson-Kubalek, E. M.; Brown, R. E.; Celia, H.; Milligan, R. A. *Proc. Natl. Acad. Sci. U.S.A.* **1998**, *95*, 8040–8045.
- (6) For an overview, see: Schnur, J. M. *Science* **1993**, *262*, 1669–1676.
- (7) For recent examples, see: D. E.; Zubarev, E. R.; Stupp, S. I. *Angew. Chem., Int. Ed.* **2002**, *41*, 1706. Sugiyasu, K.; Tamaru, S.-I.; Takeuchi, M.; Berthier, D.; Huc, I.; Oda, R.; Shinkai, S. *Chem. Commun.* **2002**, 1212.

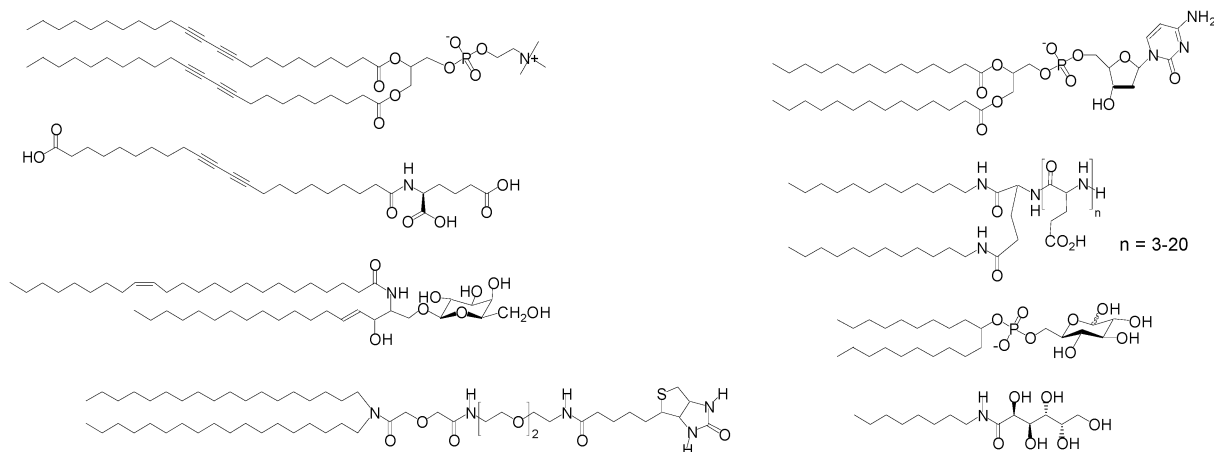


**Figure 1.** Examples of helical or twisted membrane forming amphiphiles having one or two neutral, charged or zwitterionic headgroups and one or two alkyl chains the length of which can vary from 8 to more than 20 carbons.

of the amphiphilic components.<sup>8</sup> Continuum theories invoke an intrinsic chiral bending force within the bilayer originating from the chiral packing of the molecules and/or from the chiral symmetry breaking of the bilayer associated to a collective tilt of the amphiphiles with respect to the bilayer normal. A model using a discrete description of the molecules under the form of chiral tetrahedrons has also been proposed, on the basis of an effective pair potential to express the interaction between adjacent chiral groups in a closed-packed lattice.<sup>9</sup> In any case, chiral bending relies on asymmetric interactions within the membrane itself.

A simple examination of the chemical composition of chiral membrane forming amphiphiles shows that they fulfill essential requirements for the tight packing of the molecules. They may contain very diverse functional groups, but they all have either long alkyl chains or hydrogen bonding moieties, or both, which enhance intermolecular interactions in bilayers (Figure 1). However, because of the difficulty of assessing the structures of molecules within a bilayer, detailed information about the conformations of these amphiphiles and the asymmetric molecular interactions between them have rarely been obtained.<sup>1k,10,11</sup>

Recently, interest has grown regarding the intriguing aggregation properties of a family of dimeric (“gemini”) cationic amphiphiles having the structure  $C_sH_{2s}-\alpha,\omega-(Me_2N^+C_nH_{2n+1})_2$  and referred to as  $n-s-n$ .<sup>12</sup> These amphiphiles are not chiral,

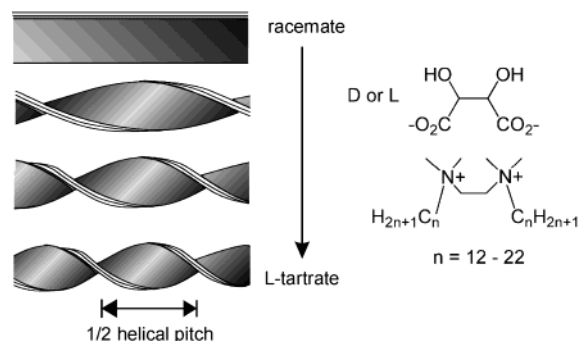


**Figure 2.** Structure of  $n-2-n$  dimeric amphiphiles having tartrate counterions and schematic representation of the multi-bilayer twisted ribbons they form in water. The pitch of the ribbons can be tuned upon varying the enantiomeric excess of the anion. The helical pitch of ribbons formed by 16-2-16 L-tartrate is 200 nm.

but in the presence of polar chiral tartrate counterions, they assemble into twisted or helical ribbons consisting of stacks of bilayer membranes, leaving very little water in the interstitial space (Figure 2).<sup>13-15</sup> Right-handed helices are formed in the presence of L-tartrate, and left-handed helices are formed with D-tartrate. That the chiral centers do not belong to the amphiphile itself but to its counterion is apparently at the origin of the two most remarkable properties of these amphiphiles. First, the width and pitch of the helices can be continuously tuned upon mixing the D and L enantiomers of tartrate in various proportions, from flat multilayer membranes for the racemate (infinite pitch) to the helices of the pure enantiomer (pitch is about 200 nm). Second, “excess chirality” can be added in the form of a sodium tartrate salt. The chiral anions are then more abundant than the amphiphilic cations, resulting in a further twist of the membrane (pitch as low as 115 nm).

Such control over the morphology and dimensions of the aggregates may be of importance in the context of possible applications of twisted or helical bilayer structures.<sup>1i,5-7</sup> With chiral amphiphiles, as shown in Figure 1, the pitch and the

- (8) For an overview of these theories, see: Selinger, J. V.; Spector, M. S.; Schnur, J. M. *J. Phys. Chem. B* **2001**, 7157–7169.
- (9) Nandi, N.; Bagchi, B. *J. Am. Chem. Soc.* **1996**, 118, 11208–16. Nandi, N.; Bagchi, B. *J. Phys. Chem. A* **1997**, 101, 1343–1351.
- (10) Diacetylenic lipids have been the most studied so far. See: Schnur, J. M.; Ratna, B. R.; Selinger, J. V.; Singh, A.; Jyothi, G.; Easwaran, K. R. K. *Science* **1994**, 264, 945–947. Thomas, B. N.; Safinya, C. R.; Plano, R. J.; Clark, N. A. *Science* **1995**, 267, 1635–1638. Spector, M. S.; Easwaran, K. R. K.; Jyothi, G.; Selinger, J. V.; Singh, A.; Schnur, J. M. *Proc. Natl. Acad. Sci. U.S.A.* **1996**, 93, 12943–12946. Spector, M. S.; Selinger, J. V.; Schnur, J. M. *J. Am. Chem. Soc.* **1997**, 119, 8533–8539.
- (11) Fuhrhop, J.-H.; Svenson, S.; Boettcher, C.; Rössler, E.; Vieth, H.-M. *J. Am. Chem. Soc.* **1990**, 112, 4307–4312. Svenson, S.; Kirste, B.; Fuhrhop, J.-H. *J. Am. Chem. Soc.* **1994**, 116, 11969–11975. Shimizu, T.; Masuda, M. *J. Am. Chem. Soc.* **1997**, 119, 2812–2818.
- (12) (a) Zana, R.; Benraou, M.; Rueff, R. *Langmuir* **1991**, 7, 1072. (b) Zana, R.; Talmon, Y. *Nature* **1993**, 362, 228–230. (c) Oda, R.; Panizza, P.; Schmutz, M.; Lequeux, F. *Langmuir* **1997**, 13, 6407. (d) Bühler, E.; Mendes, E.; Boltenhagen, P.; Munch, J. P.; Zana, R.; Candau, S. J. *Langmuir* **1997**, 13, 3096. (e) Oda, R.; Huc, I.; Candau, S. J. *Chem. Commun.* **1997**, 2105–2106. (f) Bhattacharya, S.; De, S.; *Langmuir* **1999**, 15, 3400–3401. (g) Oda, R.; Huc, I.; Homo, J.-C.; Heinrich, B.; Schmutz, M.; Candau, S. J. *Langmuir* **1999**, 15, 2384–2390. (h) Huc, I.; Oda, R. *Chem. Commun.* **1999**, 2025–2026. (i) Bernheim-Groswasser, A.; Zana, R.; Talmon, Y. *J. Phys. Chem. B* **2000**, 17, 4005. (j) Oda, R.; Huc, I.; Danino, D.; Talmon, Y. *Langmuir* **2000**, 16, 9759–9769.

- (13) Oda, R.; Huc, I.; Candau, S. J. *Angew. Chem., Int. Ed.* **1998**, 37, 2689–2691.

- (14) Oda, R.; Huc, I.; Schmutz, M.; Candau, S. J.; MacKintosh, F. C. *Nature* **1999**, 399, 566–569.

- (15) The questions of whether the bilayers are fluid or solidlike and how does their rigidity relate to the observed twisted (saddlelike) and helical (cylindrical) shapes will be the object of a full report.

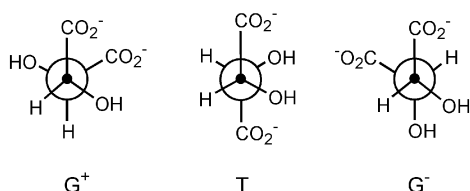


Figure 3. Main three conformers of L-tartrate.

diameter of the helices cannot be tuned in a simple way.<sup>16</sup> Unlike what we found with  $n-2-n$  tartrate amphiphiles, mixtures of enantiomers generally lead to the precipitation of the racemate<sup>1d,2a,17</sup> or to their phase separation in helices of opposite handedness.<sup>18</sup> Besides, the chiral precursors are often derived from natural products, and both enantiomers are not always readily available.

Thus far, the counterion induction of membrane chirality and continuous mixing of enantiomers have remained unique to  $n-2-n$  tartrate amphiphiles. Related systems include the counterion induced control of the helicity of helical polymers such as polyacetylene, polyaniline, polyguanidine, or polyisocyanate<sup>19</sup> and the induction of a chiral environment in micellar fibers.<sup>20</sup> The gemini tartrates are structurally less complex and more symmetric than most other chiral membrane forming amphiphiles (Figure 1). As shown in the following, their spectroscopic properties can be interpreted unambiguously to establish that the amphiphilic cations exist as a mixture of equilibrating chiral conformers in the bilayers, the population of which is dynamically controlled by a stereoselective recognition of the tartrate anions. Thus, the effect of the chiral counterions is to induce a variable degree of chirality in the bilayer. This provides an explanation for the changes of bilayer morphologies observed at a supramolecular scale and a basis for the design of new tunable membrane systems.

## Results and Discussion

**Conformation of the Tartrate Ions in Bilayers of  $n-2-n$  Amphiphiles.** Derivatives of L-tartaric acid can adopt three different conformations of the carbon chain, denoted T,  $G^+$ , and  $G^-$  (Figure 3). The anti conformation (T) is the most commonly encountered in solution and in the solid state, except for L-tartramides, which were shown to adopt gauche conformation ( $G^-$ ) in solution and in the crystal.<sup>21</sup> Tartrate salts show a strong preference for the T conformation, presumably as a result of charge repulsions. This preference is not altered by interactions of tartrate ions with 1,2-ethylenediammoniums. Indeed, all of the eleven structures of 1,2-ethylenediammonium tartrate salts

found in the Cambridge Crystallographic DataBase (CCDB) show T conformations of the tartrate.<sup>22</sup>

We assessed the conformations of tartrate ions in the chiral bilayers using circular dichroism (CD) in the absorption region of the carboxylate chromophores, at 190–250 nm (Figure 4). In aqueous solution, the CD spectrum of sodium L-tartrate is temperature independent and shows two negative bands at 194 and 211 nm. The absence of exciton coupling between the carboxylates is consistent with the expected T conformation, in which the transition moments of the two chromophores are coplanar and remote from each other, two factors that decrease coupling. Similar CD spectra are observed when sodium is replaced by micelle-forming tetraalkylammoniums, for example, cetyl-trimethylammonium (CTA), or the dimeric surfactants 12–2–12 and 16–3–16. However, the spectra are completely different when sodium is replaced by amphiphiles which assemble into chiral bilayers ( $n-2-n$  with  $n > 13$ ).<sup>12</sup> A strong negative exciton coupling between the carboxylates is then observed, with a positive peak at 202 nm and a negative peak at 219 nm. The zero of the exciton band at 209 nm matches with a maximum (shoulder) in the absorption spectrum. Such negative exciton coupling suggests a counterclockwise arrangement of the electric transition moments, as found in gauche conformation ( $G^-$ ). This is also supported by the CD spectrum of  $N,N,N',N'$ -tetramethyl L-tartramide. This compound was shown independently to adopt the  $G^-$  conformation,<sup>21</sup> and its CD spectrum shows a strong negative exciton coupling, comparable to that of tartrate, though shifted to shorter wavelengths.

Thus, L-tartrate dianions undergo a conformational change from T to  $G^-$  conformations in the chiral multi-bilayer ribbons formed by  $n-2-n$  amphiphiles. The emergence of the  $G^-$  conformations occurs only in the organized multilayer systems and not in the micelles, presumably because of a cooperative arrangement of anions and cations that results in a stronger interaction of gauche conformers with  $n-2-n$  cations. When the bilayers are heated at 50 °C above their melting temperature, a reversible transition from bilayer toward spherical micelles is observed, accompanied by a conformational change of the tartrate from  $G^-$  to T (Figure 4b).

**Conformations of  $n-2-n$  Dicationic Amphiphile Headgroups.** The  $n-2-n$  dimeric amphiphiles consist of two charged quaternary centers separated by an ethylene spacer. Both steric and electrostatic effects strongly stabilize the anti conformation of the spacer with respect to the gauche conformations. A structure search in the CCDB of hexamethyl 1,2-ethylenediammonium yielded structures which all show this anti conformation. The central ethylenediamine moiety, thus, defines a plane containing four carbons and two nitrogens (spacer plane).

Rotations about the bonds linking the nitrogens to the spacer carbons give rise to seven conformers, depending on whether the first carbon of each alkyl chain is above, below, or in the spacer plane (Figure 5). These seven conformers all include the

(16) Spector, M. S.; Selinger, J.; Singh, A.; Rodriguez, J. M.; Price, R. R.; Schnur, J. M. *Langmuir* **1998**, *14*, 3493–3500.  
 (17) Fuhrhop, J.-H.; Boettcher, C. *J. Am. Chem. Soc.* **1990**, *112*, 1768–1776.  
 (18) Singh, A.; Burke, T. G.; Calvert, J. M.; Georger, J. H.; Herendeen, B.; Price, R. R.; Schoen, P. E.; Yager, P. *Chem. Phys. Lipids* **1988**, 135–148.  
 (19) For polyacetylenes, see: Yashima, E.; Matsushima, T.; Okamoto, Y. *J. Am. Chem. Soc.* **1995**, *117*, 11596–11597; Yashima, E.; Maeda, K.; Okamoto, Y. *Nature* **1999**, *399*, 449–451. For polyisocyanates, see: Maeda, K.; Yamamoto, N.; Okamoto, Y. *Macromolecules* **1998**, *31*, 5924–5926. For polyguanidines, see: Schlitzer, D. S.; Novak, B. M. *J. Am. Chem. Soc.* **1998**, *120*, 2196–2197. For polyphosphazene, see: Yashima, E.; Maeda, K.; Yamanaka, T. *J. Am. Chem. Soc.* **2000**, *122*, 7813. For polyisocyanides, see: Ishikawa, M.; Maeda, K.; Yashima, E. *J. Am. Chem. Soc.* **2002**, *124*, 7448–7458. For polyanilines, see: Egan, V.; Bernstein, R.; Hohmann, L.; Tran, T.; Kaner, R. B. *Chem. Commun.* **2001**, 801–802 and references therein.  
 (20) Trägger, O.; Sowade, S.; Böttcher, C.; Fuhrhop, J.-H. *J. Am. Chem. Soc.* **1997**, *119*, 9120–9124.  
 (21) Gawronski, J.; Gawronska, K.; Rychlewska, U. *Tetrahedron Lett.* **1989**, *44*, 6071–6074 and references therein.

(22) Fair, C. K.; Schlemper, E. O. *Acta Crystallogr., Sect. B* **1977**, *33*, 1337. Palmer, R. A.; Ladd, M. F. C. *J. Cryst. Mol. Struct.* **1977**, *7*, 123. Perez, S. *Acta Crystallogr., Sect. B* **1976**, *32*, 2064. Perez, S. *Acta Crystallogr., Sect. B* **1977**, *33*, 1083. Aakeroy, C. B.; Bahra, G. S.; Nieuwenhuyzen, M. *Acta Crystallogr., Sect. C* **1996**, *52*, 1471. Abdou, M.; Kratky, C.; Uray, G. *Monatsh. Chem.* **1990**, *121*, 1039. Rychlewska, U. *J. Mol. Struct.* **1999**, *474*, 235. Aakeroy, C. B.; Hitchcock, P. B.; Seddon, K. R. *Chem. Commun.* **1992**, 553. Hanessian, S.; Simard, M.; Roelens, S. *J. Am. Chem. Soc.* **1995**, *117*, 7630. Gunes, B.; Soylu, H.; Akkurt, M.; Ozbey, S. *Acta Crystallogr., Sect. C* **1995**, *51*, 2346.

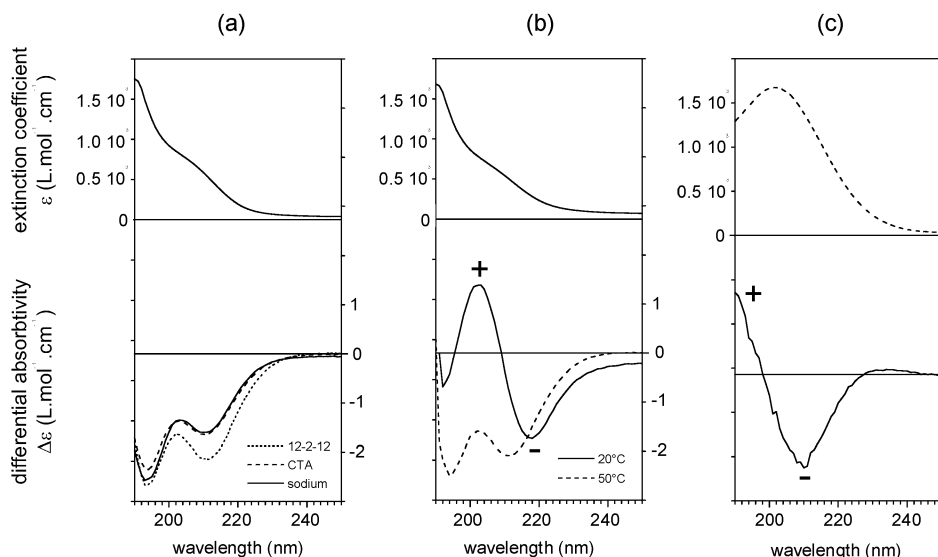


**Figure 4.** UV-vis absorption (top) and CD (bottom) spectra of carbonyl chromophores of L-tartaric acid derivatives in water at 23 °C: (a) Absorption spectrum of sodium L-tartrate and CD spectra of sodium L-tartrate, cetyl trimethylammonium (CTA), L-tartrate and 12-2-12 L-tartrate; (b) absorption spectrum of 16-2-16 L-tartrate and its CD spectra at 20 °C and 50 °C; (c) absorption and CD spectra of tetramethyl L-tartramide.

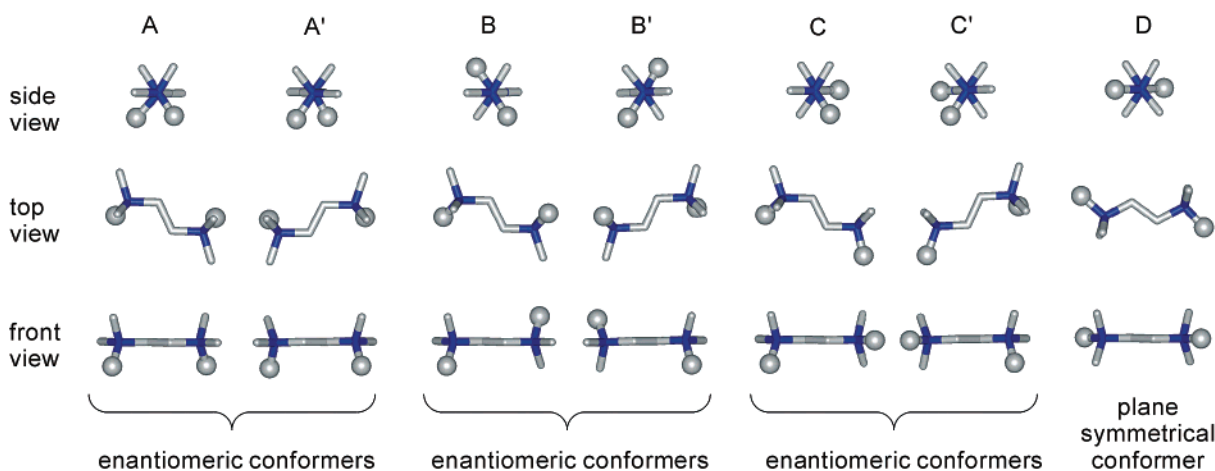
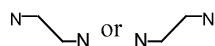


**Figure 5.** Stick representations of the seven conformers of an  $n-2-n$  dimeric amphiphile headgroup generated by  $120^\circ$  rotations about the bonds linking nitrogens (in blue) to the spacer carbons. The alkyl chains are schematized by balls. Three pairs of mirror image conformers can be defined along with plane-symmetrical conformer D. Conformers A and A' possess a  $C_2$  symmetry axis perpendicular to the spacer plane passing through the middle of the spacer C-C bond. Conformers B and B' possess an inversion center at the middle of the spacer C-C bond. All these symmetry elements are not considered with possibly different conformations of the two alkyl chains.

same number of gauche interactions, implying that they have similar energies. They can be divided into three pairs of chiral enantiomeric (mirror-image) conformers, A/A', B/B' and C/C', and one plane-symmetrical conformer, D. Enantiomeric conformers can be distinguished by the conformations of the spacer



which are chiral in the two-dimensional spacer plane (see the top view in Figure 5).

We searched for experimental evidence of the existence of these seven conformers in the solid state. Surfactants are notoriously resistant to the growth of crystals suitable for X-ray analysis. We found that our  $n-2-n$  geminis are no exception, but we, nevertheless, succeeded in obtaining the first two crystal structures in this series of long alkyl chain amphiphiles (Table 1). The 12-2-12 surfactant with bromide counterions crystallized from DMSO in the centrosymmetric  $P\bar{1}$  space group as a mixture of B and B' conformers, without any included solvent

or water molecules (Figure 6). These conformations are similar to those observed in the crystals of 4-2-4 with bromide counterions.<sup>23</sup> The spacer adopts the expected anti conformation, and the two alkyl chains extend on each side of the spacer plane. We also obtained crystals of a diacrylate derivative of 11-2-11, also having bromide counterions (Figure 6).<sup>24</sup> This compound crystallized in a dihydrate form as the D conformer. In this case, the first carbons of the alkyl chains belong to the spacer plane.

That the existence of three different conformers could be demonstrated experimentally supports the hypothesis of an equilibrium between the seven forms, of which six are chiral. In bilayers, only conformers in which both alkyl chains lie on the same side of the hydrophilic headgroup are acceptable. This is in principle possible for all A/A', B/B', C/C', and D

(23) Model compound 4-2-4 was reported to crystallize in the  $P2_1/n$  space group as a dihydrate. See: Hattori, N.; Masuda, H.; Okabayashi, H.; O'Connor, C. J. *J. Mol. Struct.* **1998**, *13*.

(24) A full report of the synthesis, aggregation properties, and polymerization of this compound is in preparation.

Table 1. Crystallographic Data

	$C_2H_4-1,2-(Br^-Me_2N^+C_{12}H_{25})_2$	$C_2H_4-1,2-(Br^-Me_2N^+C_{11}H_{22}OCOCH_2)_2$
formula	$C_{15}H_{33}BrN$	$C_{17}H_{35}BrN_2O_2 \cdot (H_2O)$
FW [g mol <sup>-1</sup> ]	307.33	397.40
crystal system	triclinic	triclinic
space group	$P \bar{1}$	$P \bar{1}$
color	colorless	colorless
unit cell parameters		
<i>a</i> [Å]	6.971	8.241
<i>b</i> [Å]	8.667	9.356
<i>c</i> [Å]	15.737	14.281
$\alpha$ [deg]	80.810	74.42
$\beta$ [deg]	88.21	85.33
$\gamma$ [deg]	66.44	71.04
temperature [K]	296	296
<i>Z</i>	2	2
<i>R</i> 1 [%]	4.7	11.2
GOF	1.034	1.036

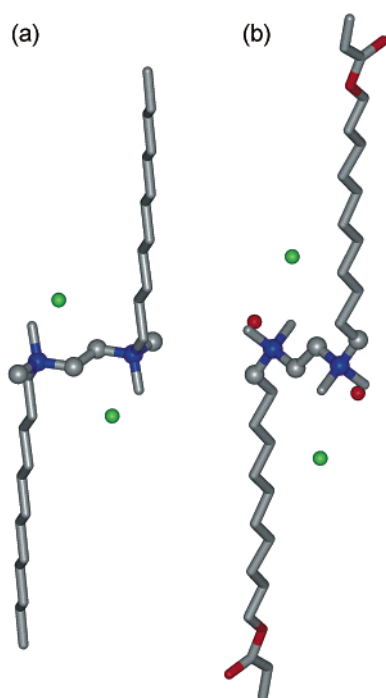


**Figure 6.** Stick representations of one of the two chiral conformers found in the crystal structures of (a) 12–2–12 and of (b) a diacrylate derivative of 11–2–11, both with bromide counterions. Hydrogens are omitted for clarity. Nitrogens are in blue, oxygens are in red, and bromides are in green. The acrylate derivative crystallized as a dihydrate. In each structure, the six coplanar atoms defining the spacer plane are shown as balls. They include two methyl groups in the structure of 12–2–12 and the first carbons of the alkyl chains in the structure of the acrylate derivative.

conformations, provided the alkyl chains are bent to point in the same direction. However, alkyl-chain bending requires high energy gauche or 1,3-diaxial conformations. The population distribution of the seven conformers is, thus, expected to be uneven. This is especially applicable at lower temperatures when the membrane is in the gel state.

Conformers A/A' are the only ones for which both chains can lie on the same side of the molecule without an additional gauche or 1,3-diaxial conformation. It seems reasonable to assume that they constitute the majority of the conformer population. An excellent representation of how A/A' conformations may look and how they may pack in bilayers is given by the crystal structure of dioctadecyl-dimethylammonium bromide

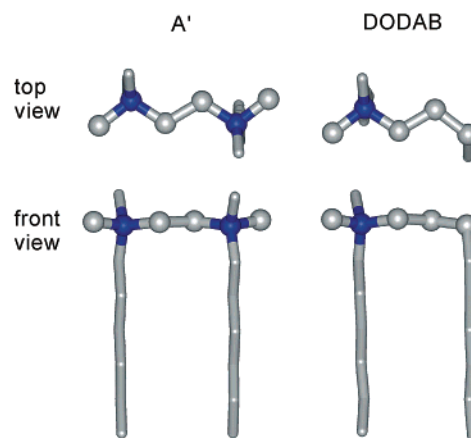
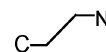


**Figure 7.** Stick representations of conformer A' of 6–2–6 and of one of the two conformers found in the crystal structure of DODAB. Hydrogens, bromides, and water molecules are omitted for clarity. The octadecyl chains of DODAB have been shortened to six and nine carbons, respectively. The balls indicate the coplanar atoms of the spacer plane.

monohydrate (DODAB).<sup>25</sup> This compound crystallized in the  $P \bar{1}$  space group as a mixture of two chiral enantiomeric conformers which can be exactly superimposed to conformers A/A', by simply replacing one dimethylammonium group of the  $n-2-n$  surfactant by a methylene group (Figure 7). In the crystal lattice, DODAB molecules pack in membrane-like bilayers (Figure 8). A bilayer contains an equal number of the two chiral conformers with their alkyl chains tilted with respect to the bilayer normal. However the chiral conformers are completely segregated in different leaflets. Each leaflet is thus composed of a single conformer, suggesting a cooperative packing arrangement of homochiral conformers. In the top view of a leaflet shown in Figure 8, the five coplanar atoms of the polar headgroups all give rise to 2D-chiral patterns of the following:



Molecules in each leaflet have opposite chiralities and are tilted in the same direction. If a single chirality is encountered in a bilayer, as might be expected with chiral counterions, one can suppose that molecules in each of the leaflets may be tilted in

(25) Okuyama, K.; Soboi, Y.; Iijima, N.; Hirabayashi, K.; Kunitake, T.; Kajiyama, T. *Bull. Chem. Soc. Jpn.* **1988**, *61*, 1485.

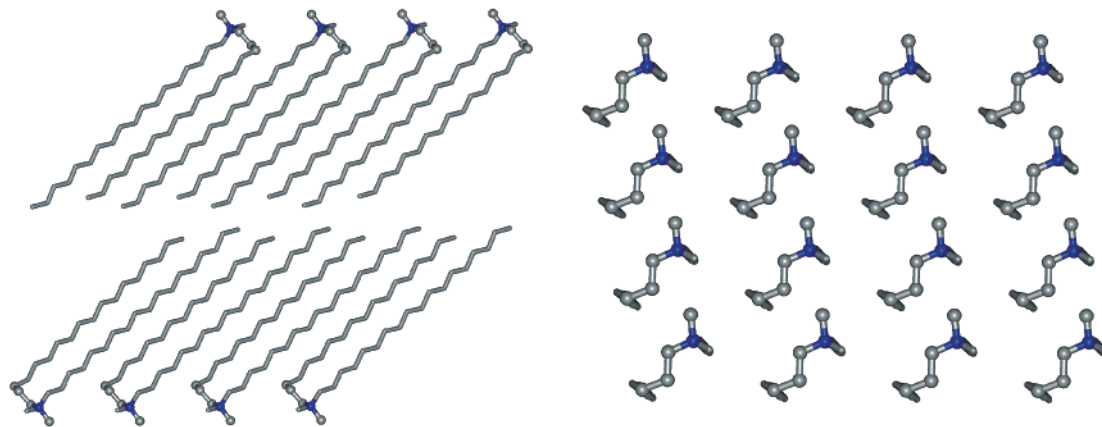


**Figure 8.** Packing arrangement of DODAB molecules in the crystal: view of a bilayer down the  $c$  crystallographic axis (left) and view of a monolayer down the direction of the alkyl chains (right). Hydrogens, bromides, and included water molecules have been omitted for clarity. The balls indicate the coplanar atoms of the spacer plane.

different directions, giving rise to a kind of polytypism as encountered in the solid-state bilayer structures of fatty acids.<sup>26</sup>

To summarize, these results show that the polar headgroups of  $n-2-n$  surfactants can adopt chiral conformations in the crystal and strongly suggest that chiral conformers are also present in bilayers. Conformers A and A' probably represent the majority of the conformer population. In the presence of bromide counterions, a bilayer is a priori equally populated in conformers of opposite chiralities (e.g., [A] = [A'], [B] = [B'], [C] = [C']). On the other hand, the balance between conformers of opposite chiralities may be expected to be shifted upon interacting with chiral counterions such as tartrate. We, thus, investigated the specific interaction between tartrates and the amphiphilic headgroups.

**Specific Recognition between  $n-2-n$  Dications and Tartrate Anions.** The formation of twisted bilayer membranes strongly depends on the structure of the amphiphile. When the  $n-2-n$  amphiphile is replaced by other cationic amphiphiles such as CTA or 16-3-16 (a homologue having a propylene spacer), the ammonium tartrates do not form twisted bilayers.<sup>14</sup> For these compounds, the CD spectra of the tartrate indicate an anti conformation similar to that of sodium tartrate (Figure 4). Conversely, when tartrate is replaced by other chiral carboxylate anions bearing hydroxy functional groups (e.g., 16-2-16 malate, glucarate, and gluconate), no twisted bilayers form either.<sup>14</sup> The formation of the twisted bilayers requires both tartrate and  $n-2-n$  cations, suggesting a specific association between the two.

We looked for indications of anion-cation recognition using  $^1\text{H}$  NMR. An aqueous solution of 12-2-12 L-tartrate below its cmc shows a sharp spectrum in which no incidence of the anion-cation interaction is detected. Both the methyls of the headgroups and two methylene units of the spacer appear as singlets, just as with bromide counterions. When the same compound is dissolved in a less polar solvent, where ionic interactions are stronger (e.g., 9:1  $\text{CDCl}_3/\text{CD}_3\text{OD}$ ),<sup>27</sup> we observed a splitting of the signals of the cationic headgroup into a diastereotopic pattern (Figure 9). The signals of the  $\text{N}^+\text{CH}_3$  appear as two singlets ( $\Delta\delta = 8$  Hz), and those of the ethylene

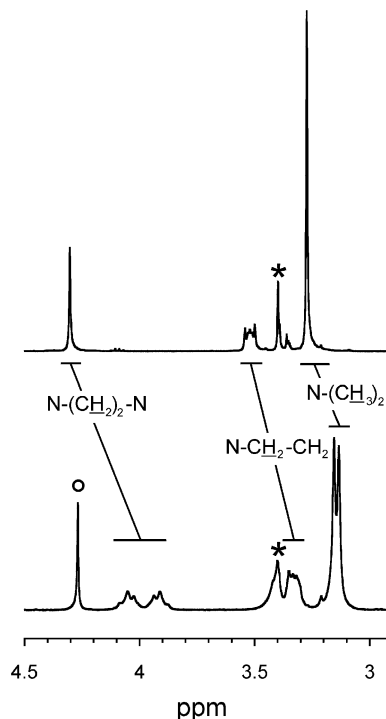


**Figure 9.** Part of the 400 MHz  $^1\text{H}$  NMR spectra of  $n-2-n$  surfactants ( $11 < n < 21$ ), 10 mM in 9:1  $\text{CDCl}_3/\text{CD}_3\text{OD}$ , with bromide counterions (top) and with tartrate counterions (bottom). The asterisks indicate the methanol residual solvent peak ( $\text{CHD}_2\text{OD}$ ). The circle indicates the  $\text{CHOH}$  signal of the tartrate counterion.

spacer appear as an AA'BB' motif ( $\Delta\delta = 68$  Hz). We also note a significant upfield shift (up to 0.3 ppm) of the signals of the protons belonging to the headgroup in the presence of tartrate ions compared to bromide ions (Figure 9).

The nonequivalence of some protons of the cation in the presence of a chiral anion demonstrates that the chiral conformers of the cation characterized in the solid state also exist in solution. Protons which are enantiotopic in a given chiral conformer of the cation become diastereotopic under the influence of a chiral anion. It also implies a close proximity between anion and cation, suggesting a tight recognition between tartrate and  $n-2-n$  dications. This recognition appears to be specific, since no such diastereotopic patterns are observed for 16-3-16 tartrate, 16-2-16 malate, 16-2-16 gluconate, or 16-2-16 glucarate. It is presumably based on matched

(26) Morishita, H.; Ishioka, T.; Kobayashi, M.; Sato, K. *J. Phys. Chem.* **1987**, *91*, 2273–2278. Amelinckx, S. *Acta Crystallogr.* **1956**, *9*, 217–224.

(27) In pure chloroform, these surfactants aggregate to form a gel, leading to an extensive broadening of the  $^1\text{H}$  NMR signals. See ref 13.

distances between the two negative charges of the dianion and the two positive charges of the dication and on their conformational properties (malate for instance differs from tartrate in conformational preference). Symmetry arguments might also be involved: all three conformers of the tartrate are  $C_2$  symmetric, and so is the central unit of the dication:



In water, the ions are solvated and the interaction is weakened compared to the case of  $CDCl_3/CD_3OD$ , but in the stacked multilayer ribbons formed by  $n-2-n$  tartrates, the anions are confined and largely desolvated between bilayers.

**Induction of Chiral Conformations in the Cationic Amphiphiles.** From the NMR data, it might be speculated that a tartrate dianion of a given chirality interacts differently with each enantiomeric conformer of the dication and modifies the balance between the two. However, NMR data show only averaged signals between these rapidly equilibrating conformers and do not allow one to assess any change in the population distribution. Moreover, the NMR measurements were performed on solutions and not on the membranes directly. In the UV-vis region,  $n-2-n$  amphiphiles have no chromophores that could indicate chiral induction. As shown in the following, vibrational CD (VCD) measurements in the absorption region of vibrators belonging to the amphiphilic cations unambiguously demonstrate that they adopt chiral conformations *in the membranes* induced by tartrate anions.

The absorption and VCD spectra of membranes of 16-2-16 tartrate and of micelles of CTA tartrate are shown in Figure 10a and b. The absorption spectra were assigned according to the absorption spectrum of sodium tartrate for the anionic moiety<sup>28</sup> and to the absorption spectrum of 16-2-16 having bromide counterions for the cationic moiety (Figure 10c). The low-frequency region between 1250 and 1800  $cm^{-1}$  is characterized by the strong antisymmetric ( $\nu_a COO^-$ ) and symmetric ( $\nu_s COO^-$ ) stretching modes of the carboxylate groups of the tartrate at 1611 and 1383  $cm^{-1}$ , respectively; by the bending modes of methyl ( $\delta CH_3$ ) and methylene ( $\delta CH_2$ ) groups of the amphiphilic cations at 1497 and 1469  $cm^{-1}$ , respectively; and by the bending mode of the CH of the tartrate at 1340  $cm^{-1}$ . In the high-frequency region, between 2800 and 3000  $cm^{-1}$ , the absorption spectra of 16-2-16 tartrate and CTA tartrate exhibit the antisymmetric ( $\nu_a CH_2$ ) and symmetric ( $\nu_s CH_2$ ) stretching modes of the methylene groups at 2917 and 2850  $cm^{-1}$ , respectively. These bands are broader and shifted to higher wavenumbers for the chains of CTA than for those of 16-2-16 because of the higher content of gauche conformations in micelles as opposed to membranes. But overall, the absorption spectra of these two compounds are similar.

In contrast, the VCD spectra of CTA L-tartrate and 16-2-16 L-tartrate reveal strong differences. The VCD spectrum of CTA L-tartrate micelles features a weak band with a bisignate line shape for the  $\nu_a COO^-$  and no band at all for the  $\nu_s COO^-$ , the  $\delta CH_2$  and the  $\delta CH_3$ .<sup>29</sup> The bisignate shape has been

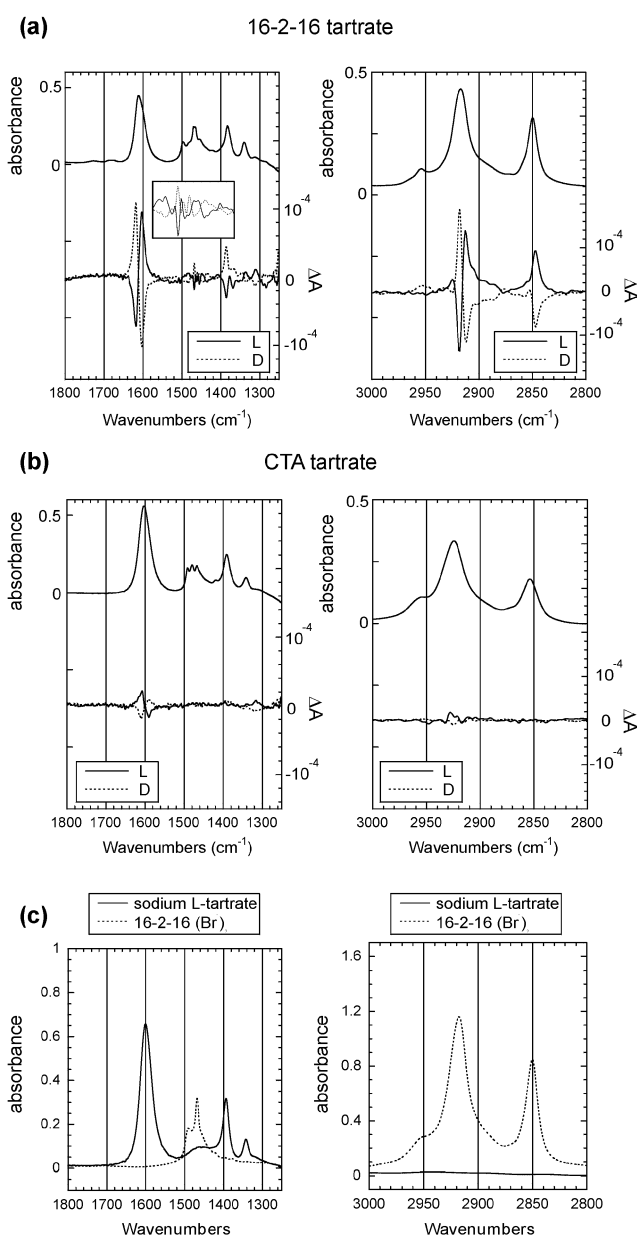


**Figure 10.** Infrared absorption and circular dichroism spectra of 16-2-16 L- and D-tartrate (a) and CTA L- and D-tartrate (b) and absorption spectra of sodium tartrate and of 16-2-16 having bromide counterions (c), recorded at 100 mM in  $D_2O$  at room temperature with a sample path length of 50  $\mu m$ . The inset of part a shows the region between 1400 and 1500  $cm^{-1}$  of the VCD spectra.

reported for tartaric acid and tartrate esters and can be explained by the exciton coupling theory.<sup>30</sup> The VCD spectrum of membranes of 16-2-16 L-tartrate also features a bisignate band for the  $\nu_a COO^-$ , but the band is more intense and its sign is opposite to that of the band of CTA L-tartrate. The spectrum also shows a weaker negative band for the  $\nu_s COO^-$  which is not seen in the spectrum of CTA L-tartrate. These differences indicate a strong conformational change of tartrate ions upon forming twisted membranes<sup>31</sup> which corroborates the results of the CD spectroscopy in the UV-vis absorption region.

(28) For a complete assignment of the IR spectrum of sodium tartrate, see: Kaneko, N.; Kaneko, M.; Takahashi, H. *Spectrochim. Acta, Part A* **1984**, *40A*, 33.

(29) For studies of the conformations of tartrate esters and tartaric acid based on the VCD spectra of the OH-stretching vibration, see: Polavaparu, P. L.; Ewig, C. S.; Chandramouly, T. *J. Am. Chem. Soc.* **1987**, *109*, 7382. Su, C. N.; Keiderling, T. A. *J. Am. Chem. Soc.* **1980**, *102*, 511. Marcott,

C.; Blackburn, C. C.; Faulkner, T. R.; Moscovitz, A.; Overend, J. *J. Am. Chem. Soc.* **1978**, *100*, 5262. Keiderling, T. A.; Stephens, P. J. *J. Am. Chem. Soc.* **1977**, *99*, 8061. Sugeta, H.; Marcott, C.; Faulkner, T. R.; Overend, J.; Moscovitz, A. *Chem. Phys. Lett.* **1976**, *40*, 397.  
(30) Holzwarth, G.; Chabay, I. *J. Chem. Phys.* **1972**, *57*, 1632. Tinoco, I. *Radiat. Res.* **1963**, *20*, 133.

Most importantly, the VCD spectrum of membranes of 16–2–16 L-tartrate features a weak negative signal for the  $\delta$  CH<sub>2</sub> at 1469 cm<sup>-1</sup> (inset of Figure 10a). A similar positive band is found in the VCD spectrum of the D-tartrate derivative, showing that this is not an artifact from the noise of the spectrum. Since tartrate ions do not absorb in this region (Figure 10c), it can be concluded that this band belongs to the cationic amphiphile and is induced by the tartrate anions.

The  $\delta$  CH<sub>2</sub> absorptions, however, are weak, and we searched for further evidence in the more intense stretching bands of the methylene groups. Indeed, the VCD spectrum of 16–2–16 with L- or D-tartrate counterions reveal very intense induced bands both for the antisymmetric ( $\nu_a$  CH<sub>2</sub> = 2917 cm<sup>-1</sup>) and for the symmetric ( $\nu_s$  CH<sub>2</sub> = 2850 cm<sup>-1</sup>) stretching. In this absorption region, CTA tartrate micelles only feature a weak VCD band at 2828 cm<sup>-1</sup> assigned to the CH stretching absorption of the tartrate ions.<sup>28</sup>

Sodium L-tartrate features a VCD spectrum almost identical to that of CTA L-tartrate (see Supporting Information), consistent with the CD spectra measured in the UV absorption region. More importantly, the micelle forming amphiphiles of the *n*-2-*n* family (e.g., 12–2–12 L-tartrate) also show the same spectrum, indicating that no chiral induction from the anion to the cation takes place in micelles when cations and anions are poorly associated. Thus, the chiral induction only takes place in membranes when cations and anions cooperatively organize in a multilayer structure.

In UV–vis CD spectroscopy, a true induced CD arises from the coupling between the transition moments of a chiral molecule and a nonchiral molecule.<sup>32</sup> Such coupling is theoretically possible for vibrational transitions<sup>30</sup> but is unlikely in the present case, owing to the large distance between the anion and the CH<sub>2</sub> vibrations of the alkyl chains and owing to the small energies associated with vibrational transitions. More commonly, induced CD signals are observed for a conformationally or a configurationally labile chirality when the equilibrium between the enantiomers is shifted in the presence of a chiral ligand (the so-called Pfeiffer effect). In view of the solid-state and NMR data which establish the existence of chiral conformers of 16–2–16 molecules in the solid and in solution, the Pfeiffer effect provides a simple explanation to the VCD signals we observe. In any case, these signals establish that 16–2–16 amphiphiles adopt chiral conformations in membranes induced by tartrate counterions.

Thus, the expression of the chirality of 16–2–16 tartrate at the supramolecular scale of the membrane probably follows a conventional mechanism. Since 16–2–16 amphiphiles are chiral in the presence of tartrate counterions, theories developed for the packing of chiral amphiphiles should a priori apply without having to invoke a direct effect of the counterions on membrane chirality. On the other hand, the originality of *n*-2-*n* amphiphiles is that their chirality is conformationally labile. Its extent will depend in a dynamic fashion upon the efficiency of the chiral induction by tartrate ions, which not only relies on the specific tartrate/amphiphile interaction but also on the

cooperative packing of the amphiphiles in the membrane. For instance, no such induction and no conformational change of tartrate ions are observed in micelles of CTA tartrate and of 12–2–12 tartrate.

This dynamic character of the chirality provides an explanation to the continuous tuning of the chiral twist we have observed in membranes of 16–2–16 L-tartrate (Figure 2). When mixing D and L enantiomers, the chiral conformational induction is expected to reflect the global enantiomeric excess. On the other hand, the amphiphiles probably pack optimally either in a racemate or in a homochiral membrane. The tartrate ions in the interstitial space between the stacked membranes also organize in a hydrogen-bonded network which is probably optimal either in a racemic or homochiral mode. The reversibility of the chiral induction should allow these opposite factors to reach a balance, which may prevent precipitation of the racemate or phase separation of enantiomers, as observed in other systems.<sup>1d,2a,17</sup> Such phenomenon bears several analogies with the interplay between locally induced chiral conformations and the long-range cooperative order, as seen in polymers.<sup>19,33</sup>

## Conclusion

The very simple and symmetrical structure of 16–2–16 tartrate amphiphiles allowed for an unambiguous interpretation of their spectroscopic features. We have demonstrated that (i) tartrate ions interact specifically with *n*-2-*n* cations; (ii) *n*-2-*n* cations exist as a mixture of chiral conformers in the solid state, in solution, and in membranes; (iii) upon forming bilayer membranes of *n*-2-*n* tartrates, tartrate ions undergo a conformational change from anti to gauche; and (iv) tartrate ions induce a shift in the population of chiral conformers of *n*-2-*n* amphiphiles, allowing the expression of molecular chirality at the supramolecular scale of the membrane.

Several questions remain open, such as the exact determination of the chiral conformers of the *n*-2-*n* (Figure 5) which interact best with D- and L-tartrate, respectively, and of the actual packing mode of *n*-2-*n* molecules in bilayers (Figure 8). Nevertheless, the results presented here highlight for the first time the consequences of the molecular phenomenon the Pfeiffer effect when expressed cooperatively at the scale of a large aggregate. They provide a sound basis for the design of new systems, where membrane chirality is tuned by chiral counterions.

Our work also represents the first application of vibrational circular dichroism to the study of chiral conformations of amphiphiles in membranes and demonstrates the very high potential of this technique which will undoubtedly develop in the future.

## Experimental Section

**Synthesis.** The *n*-2-*n* amphiphiles with bromide counterions were synthesized as described previously.<sup>12</sup> The procedure for bromide to carboxylate ion exchange was modified as follows from the initially reported use of DOWEX resin.<sup>13</sup> A suspension of the silver salt of the carboxylate in deionized water (MilliQ) was prepared freshly before each use upon mixing the corresponding acid and Ag<sub>2</sub>CO<sub>3</sub> (0.5 equiv), followed by vigorous stirring under slight vacuum for 1 h. A solution of the *n*-2-*n* surfactant (stoichiometric amount, typically 500 mg to

(31) Using ab initio quantum mechanic calculations, the signs and intensities of the VCD bands may in principle be interpreted to give a precise description of the conformation. But, this goes beyond the scope of this work and will be explored in the sequel.

(32) Ardhammar, M.; Nordén, B.; Kurucsev, T. In *Circular Dichroism: Principles and Applications, Second Edition*; Berova, N., Nakanishi, K., Woody, R. W., Eds.; Wiley-VCH Inc.: New York, 2000; pp 741–768.

(33) For a review, see: Green, M. M.; Park, J.-W.; Sato, T.; Teramoto, A.; Lifson, S.; Selinger, R. L. B.; Selinger, J. V. *Angew. Chem. Int. Ed.* **1999**, *38*, 3138–3154.



2 g scale) and the mixture were stirred for 5 min and lyophilized. The resulting powder was dissolved in MeOH and filtered on Celite to give a colorless solution. After evaporation, the product was dissolved in a mixture of chloroform/methanol (90:10), precipitated upon addition of ethyl acetate, filtered, and dried.

**Spectroscopy.** UV–vis absorption and circular dichroism measurements were performed on a Varian Cary 300 UV–vis spectrometer and a Jobin–Yvon CD6-SPEX circular dichrograph, respectively. Quartz cuvettes with optical path lengths of 2 mm (absorption) and 1 mm (CD) were used. The spectra were measured for 10 mM solutions or gels, except for *N,N,N',N'*-tetramethyl l-tartramide (1 mM). NMR spectra were recorded on a Bruker Avance 400 NB spectrometer.

Infrared absorbance and VCD measurements were performed on a Nicolet Nexus FTIR spectrometer equipped with a VCD optical bench. In this optical bench, the light beam is focused by a ZnSe lens to the sample, passing an optical filter, a Batsch wire grid polarizer, and a ZnSe photoelastic modulator which operates at 50 kHz. The light is then focused by a ZnSe lens onto a 1 mm × 1 mm liquid nitrogen cooled HgCdTe detector. The VCD spectra were recorded with 8 h data collection times at a 4 cm<sup>-1</sup> resolution. Spectra were measured in D<sub>2</sub>O at 0.1 M concentration using a calcium fluoride cell with a 50 μm Teflon spacer. In the absorption spectra, the solvent absorption was subtracted out. In the VCD spectra, the raw VCD spectrum of the solvent was subtracted.

**X-ray Diffraction Analysis.** The crystal structure of C<sub>2</sub>H<sub>4</sub>–1,2-(Br<sup>-</sup>Me<sub>2</sub>N<sup>+</sup>C<sub>12</sub>H<sub>25</sub>)<sub>2</sub> and C<sub>2</sub>H<sub>4</sub>–1,2-(Br<sup>-</sup>Me<sub>2</sub>N<sup>+</sup>C<sub>11</sub>H<sub>22</sub>OCOCHCH<sub>2</sub>)<sub>2</sub> were determined by single-crystal X-ray diffraction techniques. These crystals are mechanically fragile as well as unstable in air. During the X-ray exposures, they were sealed with part of the mother liquor in a Lindemann-glass capillary. The data were collected on a CAD4 Enraf-Nonius diffractometer with graphite monochromatized Cu Kα radiation. The cell parameters were determined by least-squares from the setting angles for 25 reflections. An empirical absorption correction was applied. The data were also corrected for Lorentz and polarization effect. The positions of non-H atoms were determined by the program

SHELXS 87, and the positions of the H atoms were deduced from coordinates of the non-H atoms and confirmed by Fourier synthesis, except for the isolated water molecules. H atoms were included for structure factor calculations but not refined.

Crystals of C<sub>2</sub>H<sub>4</sub>–1,2-(Br<sup>-</sup>Me<sub>2</sub>N<sup>+</sup>C<sub>12</sub>H<sub>25</sub>)<sub>2</sub> were grown from a supersaturated DMSO solution. In the collection of intensities, the  $\theta/2\theta$  scan method was used and 2870 independent reflections were collected in the region: 2.85° <  $\theta$  < 65.40°. Considered observed were 2863 reflections with  $I > 2\sigma I$  which were used in the subsequent calculations.

Crystals of C<sub>2</sub>H<sub>4</sub>–1,2-(Br<sup>-</sup>Me<sub>2</sub>N<sup>+</sup>C<sub>11</sub>H<sub>22</sub>OCOCHCH<sub>2</sub>)<sub>2</sub>(H<sub>2</sub>O)<sub>2</sub> were grown from the slow liquid–liquid diffusion of *n*-hexane into a chloroform solution. In the collection of intensities, the  $\theta/2\theta$  scan method was used and 1614 independent reflections were collected in the region 5.17° <  $\theta$  < 45.65°. Considered observed were 864 reflections with  $I > 2\sigma I$  which were used in the subsequent calculations. The occupancy factor of the water molecules is 85%. The poor quality of this structure is due to crystal decomposition. The low lifetime of the crystal and its weak diffraction intensity did not allow for data collection beyond  $\theta = 45^\circ$ . Nevertheless, the conclusions we draw concerning the geometry of the molecule remain valid.

**Acknowledgment.** This work was supported by the CNRS, the Universities of Bordeaux I and Bordeaux II, and by the ministry of research (predoctoral fellowship to D.B.). We thank Prof. Buss for useful advice on the interpretation of the CD data and Prof. Cuccia for proof reading the manuscript.

**Supporting Information Available:** Vibrational absorption spectra and VCD spectra of 12–2–12 L- and D-tartrate and of sodium L-tartrate. Complete coordinates for the crystal structures. This material is available free of charge via the Internet at <http://pubs.acs.org>.

JA027660J